X-602-77-89
PREPRINT

TMX 71310

ADIABATIC PARTICLE MOTION IN A NEARLY DRIFT-FREE MAGNETIC FIELD: APPLICATION TO THE GEOMAGNETIC TAIL

(NASA-TM-X-71310) ADIABATIC PARTICLE MOTION IN A NEARLY DRIFT-FREE MAGNETIC FIELD: APPLICATION TO THE GEOMAGNETIC TAIL (NASA) 42 p HC A03/MF A01 CSCL 03B
N77-24039
Unclas
G3/90 28949

DAVID P. STERN

APRIL 1977

GSFC
GODDARD SPACE FLIGHT CENTER
GREENBELT, MARYLAND

Adiabatic Particle Motion in a Nearly Drift-Free Magnetic Field: Application to the Geomagnetic Tail

David P. Stern
Theoretical Studies Group
Goddard Space Flight Center
Greenbelt, Maryland 20771

To be submitted to the Journal of Geophysical Research

ABSTRACT

The guiding center motion of particles in a 'nearly' drift free magnetic field is analyzed in order to investigate the dependence of mean drift velocity on equatorial pitch angle, the variation of local drift velocity along the trajectory and other properties. Consider a 2-dimensional magnetic field $\underset{\sim}{B}$, somewhat resembling the field of the geomagnetic plasma sheet, which has the following properties: (1) No y component and no y dependence (2) $B_x = 0$ in the equatorial plane $z = 0$ and (3) $B_z = B_o$ = constant. In such a field, , it has been shown, particles may be trapped, but they exhibit no net drift in the y direction: their instantaneous drifts at any time may be large, but when they are averaged over a sufficiently long time (or, for adiabatic particles, over a bounce period) the result is zero. Here a slight modification of this mode is explored -- motion in a field in which B_z slowly varies in the x direction, as is indeed observed in the geomagnetic tail. The mean drift $\langle v_y \rangle$ for adiabatic particles can now be expressed by means of elliptic integrals: it no longer vanishes but is merely small -- if v_o is the drift velocity for equatorial particles (which is easily derived), $\langle v_y \rangle$ is typically between v_o and $v_o/3$. By contrast, instantaneous guiding center drift velocities at $z = 0$ may be 50 times larger. Explicit approximations to the twice-averaged Hamiltonian $W(\alpha, \mu, J)$ near $z = 0$ are also derived, permitting simple representation of drift paths if an electric potential $\phi(\alpha, \beta)$ also exists. In addition, the use of W or of expressions for the longitudinal invariant allows the derivation of the twice averaged Liouville equation and of the corresponding Vlasov equation. Bounce times are calculated (using the drift-free approximation), as are instantaneous guiding center drift velocities, which are then used to provide a numerical check on the formulas for $\langle v_y \rangle$.

INTRODUCTION

It has been shown [Stern and Palmadesso, 1975] that in two-dimensional magnetic fields of the form

$$\underset{\sim}{B} = B_x(z)\,\hat{\underset{\sim}{x}} + B_z\,\hat{\underset{\sim}{z}} \qquad (1)$$

(B_z a non-zero constant, $B_x(0) = 0$) charged particles trapped in the vicinity of the equatorial plane $z = 0$ where the field intensity is weakest do not experience any net magnetic drift in the y direction. In the guiding center mode of motion, such particles do experience a non-zero curvature and/or gradient drift at any point of their trajectory. However, when the effects of such drifts are summed up over one entire bounce period between mirror points, it is found that independently of the strength B_m of the mirror-point field, the net effect of all such drifts cancels out, so that the guiding center merely wobbles back and forth in the neighborhood of one fixed guiding field line (Figure 1).

The field (1) is not curl-free and thus is not expected to be formed in space plasmas, since a net transport of charge is required for maintaining it [Stern and Palmadesso, 1975]. However, there do exist fields which deviate only moderately from (1) -- in the plasma sheet of the earth's magnetosphere, in the Jovian magnetodisk, in "spiked helmet" configurations in the solar corona [Schatten, 1971] and possibly in the large-scale structure of the interplanetary magnetic field [Smith et al., 1976]. In such "nearly drift free" fields the net drift of particles is not zero but merely small, so that a relatively high plasma density can be contained in them without creating too high a current density, which might disrupt the magnetic geometry. Thus nearly drift free fields may be nature's way of containing high-β

plasmas effectively, and perhaps this is the reason why they seem to occur as frequently as has been observed.

The purpose of this work is to analyze guiding center motion in what may well be the simplest type of a nearly drift free field, namely the field

$$\underset{\sim}{B} = \frac{1}{2}\lambda z \ \underset{\sim}{\hat{x}} + (B_0 + \frac{1}{2} k x) \ \underset{\sim}{\hat{z}} \qquad (2)$$

where

$$k/\lambda = \varepsilon \ll 1$$

In such a field, as will be seen, :acteristic quantities such as bounce times, longitudinal invariants and mean drift rates are readily expressed in terms of elliptic integrals, and appendix A develops some of the mathematical tools required for handling them.

One questions which this study answers concerns the dependence of mean drift velocities on equatorial pitch angle. For particles in the field (2) confined to the equatorial plane $z = 0$ the mean drift velocity v_y (which equals the gradient drift experienced there -- see Stern and Palmadesso [1975], equation 7) is readily computed. How does v_y vary as the equatorial pitch angle is decreased? The results derived here (see Table 1) suggest that the variation is relatively slow, so that for many purposes results obtained for $z = 0$ can be used as a crude approximation.

The study also shows that although the average drift velocity of particles in such fields is slow, the curvature and gradient velocities observed at different points along their trajectory may be quite large. Thus if a distribution of such particles is observed only in some selected region along their trajectories -- e.g., near the equatorial plane -- misleading values for their average bulk velocity could be deduced.

THE LONGITUDINAL INTEGRAL

Consider a somewhat more general two-dimensional field which includes both (1) and (2) as special cases

$$\underset{\sim}{B} = B_x(z)\,\hat{\underset{\sim}{x}} + B_z(x)\,\hat{\underset{\sim}{z}} \tag{3}$$

where we assume as before that $B_x(0) = 0$ and that the field is weakest at $z = 0$, so that trapping can occur. Introducing Euler potentials (α, β)

$$B = \nabla\alpha \times \nabla\beta \tag{4}$$

a convenient choice of these functions is provided by

$$\alpha = \int B_z\,dx - \int B_x\,dz \tag{5a}$$

$$\beta = y \tag{5b}$$

We now define the longitudinal integral I for a particle with kinetic energy W and mirroring field intensity B_m by means of

$$\begin{aligned} J &= (2mW)^{1/2} \oint (1 - B(z)/B_m)^{1/2}\,ds \\ &= (2mW)^{1/2}\, I \end{aligned} \tag{6}$$

with integration performed along a field line between mirror points. Along a field line

$$\frac{ds}{B} = \frac{dz}{B_z} = \frac{dx}{B_x} \tag{7}$$

and hence

$$I = \oint (1 - B/B_m)^{1/2}(B/B_z)\,dz \tag{8}$$

However, calculations are considerably simplified if z is replaced as integration variable by the field magnitude B . From (3)

$$B^2 = B_x^2(z) + B_z^2(x) \tag{9}$$

Hence along a field line, using (7) and assuming independent variables (α, z)

$$B\,dB = \left[B_x\, dB_x/dz + B_z(dB_z/dx)(\partial x/\partial z)\big|_\alpha \right] dz$$

$$= B_x\,(dB_x/dz + dB_z/dx)\, dz \tag{10}$$

Thus

$$I = \oint \frac{(1 - B/B_m)^{1/2}\, B^2}{B_z\, B_x(dB_x/dz + dB_z/dx)}\, dB \tag{11}$$

THE LIMIT $\varepsilon \to 0$

Quantities such as I derived for (2) will differ only by corrections of order ε from their values for the drift-free limit $\varepsilon = 0$. The calculation will thus begin with an analysis of that limit, using

$$B_z = B_o = \text{constant} \tag{12a}$$

$$B^2 = \lambda^2 z^2/4 + B_o^2 \tag{12b}$$

$$B_x(dB_x/dz) = \tfrac{1}{2} \lambda\, (B^2 - B_o^2) \tag{12c}$$

$$I = (8/\lambda B_o B_m^{1/2}) \int_{B_o}^{B_m} \frac{(B_m - B)^{1/2}\, B^2\, dB}{(B^2 - B_o^2)^{1/2}} \tag{13}$$

Here we have assumed for simplicity $B_x(z) = - B_x(-z)$; in the absence of such symmetry, I will be proportional to the sum of two integrals of the form (13), one for $z > 0$ and the other for $z < 0$. The calculation then proceeds as outlined below and leads to similar conclusions, but I everywhere contains the sum of two distinct integrals. In the present case the integral depends on two independent parameters B_o and B_m , but only one such parameter remains if B is replaced by the dimensionless variable u :

$$u = B/B_o \qquad (14a)$$

$$u_m = B_m/B_o \qquad (14b)$$

Then

$$I = (8\, B_o/\lambda\, u_m^{1/2}) \int_1^{u_m} \frac{u^2 \; (u_m - u)^{1/2}}{(u^2 - 1)^{1/2}} \, du$$

$$= (8\, B_o/\lambda u_m^{1/2}) \;\; S_2(u_m) \qquad (15)$$

where S_2 is expressible in terms of elliptic integrels <u>K</u> and <u>E</u> of the argument m , where $m^2 = (u_m-1)/(u_m+1)$ (see appendix A), namely

$$S_2 = (2/15)\, (u_m+1)^{1/2} \left[\underline{E}\, (2\, u_m^2 - 9) + \underline{K}\, (9 - 2\, u_m) \right] \qquad (A\text{-}10)$$

THE HAMILTONIAN W FOR $\varepsilon = 0$

For some applications it is useful to express the kinetic energy W in terms of (J, μ, α, β), a procedure which makes it possible to write down a Hamiltonian for the twice-averaged motion [<u>Northrop</u> <u>and</u> <u>Teller</u>, 1960 ; <u>Chen</u> <u>and</u> <u>Stern</u>, 1975]. Substituting (6) in (15) gives

$$J/(2mW)^{1/2} = (8\, B_o/\lambda\, u_m^{1/2})\; S_2(u_m) \qquad (16)$$

One now substitutes on the left

$$W = \mu\, B_m = \mu\, u_m\, B_o \qquad (17)$$

giving

$$J\,\mu^{-1/2} = N\,S_2(u_m) = N\,S_2(W/\mu\,B_0) \tag{18}$$

where

$$N = 8\,(2\,m\,B_0^3)^{1/2}/\lambda = \text{constant} \tag{19}$$

Equation (18) clearly shows that W is independent of (α,β), as is required for the drift-free property of the field in the limit $\varepsilon = 0$. Furthermore, in this limit the dependence of W on μ and J may be expressed by a function of a single variable -- namely, W/μ depends only on the single variable $F = J\,\mu^{-1/2}$: this property is common to geometries free from electric fields, as was shown by Taylor [1964].

The functional form of W is defined by the integral relation (6) and in order to extract it explicitely that relation must be inverted, which tends to be a difficult task. Fortunately, the most significant applications of W only require its derivatives, which through the canonical equations of motion [Northrop and Teller, 1960, eqs. 30] give the bounce averaged drift rates and which also, through Liouville's theorem, allow the twice-averaged Vlasov equation to be expressed. These derivatives are most easily obtained by implicit differentiation of (6), and this is the line which will be adopted in deriving the mean drift velocities when $\varepsilon \neq 0$.

The explicit form of W is required mainly for deriving contours of constant Hamiltonian K [Northrop and Teller, 1960]. In a time-independent magnetic field for which W is known and where an electric field orthogonal to B is present and is expressed by its scalar potential $\Phi(\alpha,\beta)$, such contours are easily drawn and provide a quick visualization of the motion of charged particles through the given configuration. Chen and Stern [1975] derived the limiting forms of W for a dipole field in the limits $J = 0$ (equatorial) and $\mu = 0$, and proceeded to bridge these two extreme cases for intermediate values of (J, μ) with an analytical approximation accurate within 1% . Here only the form of W for near-equatorial particles will be developed.

In the limit $J = 0$, (17) gives

$$W = \mu B_o \tag{20}$$

Consider next a particle with a small but nonzero value of J ; in that case it is useful to introduce a new variable w

$$w = u - 1 \tag{21a}$$

$$w_m = u_m - 1 = (W/\mu B_o) - 1 \tag{21b}$$

$$S_2(u_m) = \bar{S}_2(w_m) \tag{21c}$$

and to denote for convenience

$$F = J\,\mu^{-1/2} \tag{22}$$

Then (18) gives

$$F/N = \bar{S}_2(W/\mu B_o - 1) \tag{23}$$

and one sees that in order to obtain $W(\mu, J)$ in explicit form it is required to invert the function $\bar{S}_2$. To lowest order (obtained either by approximating the integral in (15) for small values of w_m or by inserting appropriate series expansions of $\underline{E}$ and $\underline{K}$ in equation A-10) one finds

$$\bar{S}_2(w_m) \approx (\sqrt{2}\,\pi/4)\;w_m \tag{24}$$

leading to

$$W \approx \mu B_o \left[1 + (2\sqrt{2}/\pi)\ F/N\right] \qquad (25)$$

Equation (24) also leads to the approximation

$$I \approx (2\sqrt{2}\pi/\lambda)(B_m - B_o) \qquad (26)$$

which for the geometry discussed here forms the counterpart of an approximation devised by Schulz [1971 ; eq. 10] for I in the dipole field. Using additional terms in the expansions of $\underline{K}$ and $\underline{E}$ gives as generalization of (24)

$$\bar{S}_2 \approx (\sqrt{2}\pi/4)\left[w + (7/16)\,w^2 + (19/256)\,w^3\right] \qquad (27)$$

Neglecting the last term and inverting the relation which remains then gives

$$W \approx \mu B_o \left\{1 + (8/7)\left[(1 + 1.5756\,J\,\mu^{-1/2}/N)^{1/2} - 1\right]\right\} \qquad (28)$$

where N is the constant given by (19). This relation is accurate to about 1% up to $u_m \approx 1.5$.

THE BOUNCE TIME

The time for one full back-and-forth oscillation, evaluated in the limit $\varepsilon = 0$ by the same methods as those used for I , is

$$\tau = \oint \frac{ds}{v_{\parallel}}$$

$$= (8 B_0 u_m^{1/2} / \lambda v) \int_1^{u_m} \frac{u^2 \, du}{(u_m - u)^{1/2} (u^2 - 1)^{1/2}} \qquad (29)$$

The integral expressed here will be denoted by I' and one easily sees that

$$I' = 2 \, dS_2 / du_m \qquad (30)$$

(compare Schulz [1971] , eq. 7). To evaluate I' it is best to split it into two parts

$$I' = \int \left(\frac{u^2 - 1}{u_m - u} \right)^{1/2} du + \int \frac{du}{(u_m - u)^{1/2} (u^2 - 1)^{1/2}}$$

$$= I_1 + I_2 \qquad (31)$$

Integrating by parts, one finds that I_1 reduces to one of the class of integrals analyzed in appendix A , namely

$$I_1 = 2 S_1 \qquad (32)$$

The second integral may be handled by standard substitutions which lead to elliptic integrals (e.g. Milne-Thomson [1964] , page 597) and is given by

$$I_2 = 2\,(u_m + 1)^{1/2}\,\underline{K}(m) \qquad (33a)$$

where $\underline{K}$ is a complete elliptic integral of the first kind and its argument m (which also appears in the terms of eq. 32) satisfies

$$m^2 = (u_m - 1)/(u_m + 1) \qquad (33b)$$

A tabulation of $T = 2\,u_m^{1/2}\,I'$ is given in table 1 . The conversion of these values to actual time intervals requires multiplication by $4\,B_o/\lambda v$; in conditions appropriate to the earth's magnetotail

$$B_o/\lambda \approx 1\,R_e$$

and for 1 keV protons T turns out to be approximately equal to τ in minutes. For 1 keV electrons, 1.36 T approximates τ in seconds.

NORMALIZED CALCULATION FOR $\varepsilon \neq 0$

Before calculating the motion of charged particles in the field (2) , it is useful to transform the equations to dimensionless form, since that reduces the number of independent variables and therefore allows the same result to be used for a large variety of situation . Such transformations are usually accomplished by scaling -- e.g. dividing all distances by a scale length. In the present system a natural scale length is

$$L = B_o/\lambda \qquad (34)$$

One can visualize L as follows. In the limit $\varepsilon = 0$ any field line follows a parabola

$$\alpha = -\lambda z^2/4 + B_o x = \text{constant} \qquad (35)$$

Along this parabola the direction of B gradually rotates from being orthogonal to the x axis to being parallel to it. The point at which B has rotated by 45° -- half its total rotation range -- occurs when $B_x = B_z$ and is L/2 above or below the equatorial plane. As noted at the end of the preceding section, in the earth's magnetotail $L \approx 1 R_E$. We now use L to define scaled distances

$$\zeta = z/L \tag{36a}$$

$$\xi = x/L \tag{36b}$$

and also introduce a scaled magnetic field

$$\underset{\sim}{u} = \underset{\sim}{B} / B_o \tag{37a}$$

and a scaled Euler potential

$$\alpha' = \alpha / B_o L \tag{37b}$$

The dependence of ζ and $|\underset{\sim}{u}|$ on ξ is depicted in Figure 2 .
With these variables, the basic relations become

$$\underset{\sim}{u} = \frac{1}{2} \zeta \, \hat{\underset{\sim}{x}} + \left(1 + \frac{1}{2} \varepsilon \xi \right) \hat{\underset{\sim}{z}} \tag{38}$$

$$\alpha' = \xi + \varepsilon \xi^2/4 - \zeta^2/4 \tag{39}$$

$$\partial B_x / \partial z = \lambda \, \partial u_x / \partial \zeta \tag{40a}$$

$$\partial B_z / \partial x = \lambda \, \partial u_z / \partial \xi \tag{40b}$$

Substituting in (11)

$$I = 4L \int_{u(0)}^{u_m} \frac{(1 - u/u_m)^{1/2} \; u^2 \, du}{u_z \, u_x \, (du_x/d\zeta + du_z/d\xi)} \tag{41}$$

From (38) the sum in the denominator is simply $(1+\varepsilon)/2$. The components of $\underset{\sim}{u}$ are also easily derived, but their functional dependence must be transformed from (ξ, ζ) to (u, α') in order to suit the integration. If terms of order ε^2 or smaller are neglected, one finds

$$u^2 \approx \zeta^2/4 + 1 + \varepsilon\xi$$

$$\approx \zeta^2/4 + 1 + \varepsilon(\alpha' + \zeta^2/4) \quad (42)$$

$$(1+\varepsilon)\, u_x^2 \approx u^2 - 1 - \varepsilon\alpha'$$

$$u_x \approx (u^2 - 1 - \varepsilon\alpha')^{1/2}\,(1+\varepsilon)^{-1/2} \quad (43)$$

From (38), (39) and (43), using (39) only to lowest order

$$u_z \approx 1 + \varepsilon\xi/2$$

$$\approx 1 + (\varepsilon/2)(\alpha' + u_x^2)$$

$$\approx 1 + (\varepsilon/2)(\alpha' + u^2 - 1) \quad (44)$$

Substituting everything in (41) one obtains the form of I to order ε as

$$I = \psi\, u_m^{-1/2} \int_{u_o}^{u_m} \frac{(u - u_m)^{1/2}\; u^2 \; du}{\left[1 + (\varepsilon/2)(\alpha' + u^2 - 1)\right]\,(u^2 - 1 - \varepsilon\alpha')^{1/2}} \quad (45)$$

where

$$u_o^2 = 1 + \varepsilon\alpha' \quad (46a)$$

$$\psi = 8L\,(1+\varepsilon)^{-1/2} \quad (46b)$$

Note that the dependence on α' must be preserved even if we choose to deal with the field line $\alpha' = 0$, since $\partial I/\partial \alpha'$ is required in the calculation of mean drift velocities. Introducing a new variable w (not related to w in equation 21) through

$$w^2 = u^2 - \varepsilon \alpha' \qquad (47a)$$

$$w_m^2 = u_m^2 - \varepsilon \alpha' \qquad (47b)$$

we get

$$u \approx w \left[1 + \varepsilon(\alpha'/2w^2) \right] \qquad (48)$$

$$u_m - u \approx (w_m - w) \left[1 - \varepsilon(\alpha'/2\, w\, w_m) \right] \qquad (49)$$

Thus to order ε

$$I = \frac{\psi}{u_m^{1/2}} \int_1^{w_m} \frac{(w_m - w)^{1/2}\, w^2}{(w^2 - 1)^{1/2}} \left[1 + \varepsilon \left(\frac{\alpha'}{2\, w^2} - \frac{\alpha'}{4\, w\, w_m} - \frac{\alpha' + w^2 - 1}{2} \right) \right] dw$$

$$= \frac{\psi}{u_m^{1/2}} \left[S_2(w_m) + \varepsilon \left(\alpha' S_0/2 - \alpha' S_1/4\, w_m - (\alpha' - 1) S_2/2 - S_4/2 \right) \right]$$

(50)

where the S_k are integrals defined in appendix A

$$S_k(u_m) = \int_1^{u_m} \left(\frac{u_m - u}{u^2 - 1} \right)^{1/2} u^k \, du \qquad (A-1)$$

Now let I' be defined by

$$I = u_m^{-1/2}\, I' \qquad (51)$$

By (6)

$$J = (2\, m\, \mu\, B_o)^{1/2}\, I'(\alpha', w_m) \qquad (52)$$

where by (47b)

$$w_m = w_m(u_m, \alpha') = w_m(W/\mu B_o, \alpha') \qquad (53)$$

The last two relations implicitely express the functional relationship

$$W = W(\alpha, \mu, J) \qquad (54)$$

Differentiating by α'

$$0 = \frac{\partial \alpha'}{\partial \alpha} \frac{\partial I'}{\partial \alpha'} + \frac{\partial I'}{\partial w_m} \left(\frac{1}{\mu B_o} \frac{\partial w_m}{\partial u_m} \frac{\partial W}{\partial \alpha} + \frac{\partial w_m}{\partial \alpha} \right) \qquad (55)$$

Only errors of higher order are committed if we set both ψ and $\partial w_m/\partial u_m$ equal to 1 and if we evaluate (in the expression below) $\partial I'/\partial w_m$ only to the lowest order. This gives

$$\frac{\partial W}{\partial \alpha} \approx \frac{-\mu}{dS_2/du_m} \quad \frac{\partial I'}{\partial \alpha'} + \frac{dS_2}{du_m} \frac{\partial w_m}{\partial \alpha'} \qquad (56)$$

From (48)

$$\partial w_m/\partial \alpha' \approx -\, \varepsilon/2\, u_m \qquad (57)$$

hence

$$\frac{\partial W}{\partial \alpha} = -\, \frac{\varepsilon\, \mu\, L}{dS_2/du_m} \left[S_0/2 - S_1/4\, u_m - S_2/2 - (dS_2/du_m)/2\, u_m \right] \qquad (58)$$

SCALING OF DRIFT VELOCITY AND TIME

An independent numerical integration of guiding center drifts in the field (2) was performed which served as a check on the analytical formula (58) and which also provided information about the mean drift velocity in various portions of the orbit and about the time spent by the particle in these portions. In performing these numerical checks some additional scaling was introduced, in the following way.

The mean drift velocity $\langle v_y \rangle$ may be derived from (58) by the relation

$$q \langle v_y \rangle = \frac{\partial W}{\partial \alpha} = - \frac{\varepsilon \mu \lambda}{B_o} f(u_m) \qquad (59)$$

where $f(u_m)$ is the function defined by (58) ; note that since $\partial W/\partial \alpha$ is expressed in terms of the derivatives of I (see eq. 55) , we are actually using equations (27) of Northrop and Teller [1960] , rather than equations (30) there. Let a scaling velocity v_o be defined

$$v_o = 4 k m v^2 / q B_o^2 \qquad (60)$$

As will be seen below (equation 72), v_o is the gradient drift velocity for equatorial particles $(J = 0)$, also given by equation (7) of Stern and Palmadesso [1975] . By (59)

$$v_y = - 2 v_o f(u_m)/u_m \qquad (61)$$

One may also devise a "scale time" t_o for the bounce motion

$$t_o = L/v = B_o/\lambda v \qquad (62)$$

so that (29) becomes

$$\tau = 8\, t_o\, u_m^{1/2} \int_1^{u_m} u^2 \left[(u_m - u)(u^2 - 1)\right]^{-1/2} du \qquad (63)$$

Table 1 lists $\langle v_y \rangle / v_o$ and $\tau/4t_o$ for selected values of u_m, obtained by means of (58) and (63), and Figures 3 and 4 represent these functions graphically.

Let v_y (without averaging brackets) be the guiding center drift velocity of particles with given v_o and u_m, computed for various points of the trajectory. For such particles

$$\langle v_y \rangle \tau = \oint v_y\, dt \qquad (64)$$

This relation allows $\langle v_y \rangle$ to be derived numerically, but one must proceed with caution, because the integral has to be evaluated to an accuracy of the first order in ϵ. Transforming the integration variable by means of a zero-order relation between t and some other variable (e.g. u or z) may lead to a finite error even if v_y in the integrand is given correctly to order ϵ. One may, however, us (7), which is exact, to obtain

$$\langle v_y \rangle = \oint (v_y / v_{\parallel})\, ds$$

$$= \frac{4\, u_m^{1/2}}{v} \int_0^{z_m} \frac{v_y\, u\, dz}{u_z\, (u_m - u)^{1/2}} \qquad (65)$$

where z_m corresponds to the mirror point. Note that at the upper limit the integrand diverges, so that a different mode of numerical integration may be required for the vicinity of the mirror point: one convenient device for accomplishing this is described in appendix B .

THE DRIFT VELOCITY

All guiding center drifts in the field (2) are in the $\hat{\underset{\sim}{y}}$ direction and therefore can be added or subtracted algebraically. This follows from the observation that the components constituting these drifts (see below) are aligned either with $\underset{\sim}{B} \times \nabla B^2$ or with $\nabla \times \underset{\sim}{B}$. In the first case

$$\underset{\sim}{B} \times \nabla B^2 = \hat{\underset{\sim}{y}} \left(- \lambda^3 z^2/4 + B_0^2 k \right)$$

$$= \hat{\underset{\sim}{y}} \lambda B_0^2 \left(- \zeta^2/4 + \varepsilon \right) \tag{66}$$

and in the second one

$$\nabla \times \underset{\sim}{B} = \hat{\underset{\sim}{y}} (\lambda/2)(1 - \varepsilon) \tag{67}$$

The two principal components of $\underset{\sim}{v}_y$ are the gradient drift

$$\underset{\sim}{v}_g = (v_\perp^2 /2\omega B^2)(\underset{\sim}{B} \times \nabla B) \tag{68}$$

and the curvature drift

$$\underset{\sim}{v}_c = (v_\parallel^2 /\omega B) \; \underset{\sim}{B} \times (\hat{\underset{\sim}{B}} \cdot \nabla \hat{\underset{\sim}{B}})$$

$$= (v_\parallel^2 /\omega B) \left[(\nabla \times \underset{\sim}{B}) + \hat{\underset{\sim}{B}} \times \nabla B \right] \tag{69}$$

where $\omega = qB/m$ is the gyration frequency. Then by (60)

$$v_\perp^2 /2\omega B^2 = 2 v_0/(k \, u_m \, u \, B) \tag{70}$$

$$v_\parallel^2 /\omega B = 4(v_0/ku^2)(1 - u/u_m) \tag{71}$$

Thus

$$v_g = \frac{v_0}{\varepsilon} \frac{1}{u_m u^3} \left(- \frac{\zeta^2}{4} + \varepsilon \right) \tag{72}$$

$$v_c = 2\frac{v_0}{\varepsilon}\left(1 - \frac{u}{u_m}\right)\left[\frac{1-\varepsilon}{u^2} + \frac{1}{u^2}\left(-\frac{\zeta^2}{4} + \varepsilon\right)\right] \qquad (73)$$

These results may now be inserted in (65) to obtain a numerical estimate of $\langle v_y \rangle$. Note that although v_y may be separated in (72) and (73) into parts of order v_0 and v_0/ε , the contribution of the latter part to $\langle v_y \rangle$ does not vanish but is merely of order v_0 , because the integration path differs slightly from its limit for $\varepsilon = 0$. This prevents one from calculating $\langle v_y \rangle$ through (65) by summing up terms of the same order and instead, one must include terms of lower order , the contributions of which almost (but not completely) cancel out.

This in its turn demands a computing accuracy exceeding by a factor $1/\varepsilon$ the accuracy of the final result: the advantage is that a relatively simple formula (65) can be used, avoiding the cumbersome transformations which lead to (58). In practical evaluations, the numerical result agreed within a few percent with (58); as an additional check, the time was also integrated numerically, and the results were compared with (29).

Table 2 contains a sample result for a field with $\varepsilon = 0.01$, for particles mirroring at $\zeta = 1.4$, $u_m = 1.2227$. The fourth column tabulates values of the integrand of (65), multiplied by the step size $\Delta z = 0.05$ (for brevity, only every alternate step is tabulated). while the 5th column gives the integrand of (63), multiplied by $2\, u_m^{1/2}\, \Delta z$. Analytical and numerical results for the total displacement and time (equator to mirror point) are listed, and the displacements obtained analytically are shown in Figure 5 . Note that the displacement is negative near the equator, where curvature drift dominates, but is positive near the mirror points (the net drift is also positive). Note also that the drift velocity deduced for the point at the top of the table is about 50 times larger, and in the opposite direction, than the

A certain amount of caution should be excercised when the preceding results are applied to observations, because the average drift velocity will not in general equal the plasma's bulk velocity $\underset{\sim}{V}$ orthogonal to the magnetic field $\underset{\sim}{B}$. To emphasize this point, consider the current density $\underset{\sim}{j}_{\perp}$ carried in a direction orthogonal to $\underset{\sim}{B}$ by a plasma of particles of a single kind only, e.g. electrons. If at any given point f is the distribution function of such particles and n their density, then their bulk velocity is

$$\underset{\sim}{V}_{\perp} = (1/n) \int \underset{\sim}{v}_{\perp}\, f \; d^3\underset{\sim}{v}_{\perp} \tag{74}$$

and

$$\underset{\sim}{j}_{\perp} = n\, q\, \underset{\sim}{V}_{\perp} \tag{75}$$

On the other hand, if $\langle \underset{\sim}{v}_d \rangle$ is the mean guiding center velocity and M the magnetic moment density, then

$$j = n\, q \langle \underset{\sim}{v}_d \rangle + \nabla \times \underset{\sim}{M} \tag{76}$$

Unless $\nabla \times \underset{\sim}{M}$ vanishes $\langle \underset{\sim}{v}_d \rangle$ will in general differ from $\underset{\sim}{V}_{\perp}$. In particular, one can envision static equilibria in which the plasma distribution function is everywhere isotropic: by (74) $\underset{\sim}{V}_{\perp}$ and $\underset{\sim}{j}_{\perp}$ both vanish, but $\langle \underset{\sim}{v}_d \rangle$ may be quite large.

As a concrete example, let $\underset{\sim}{B} = B(x, y)\, \hat{\underset{\sim}{z}}$, n = constant and let all particles have the same $v_{\perp}$. Then no curvature drift exists and all particles share the same gradient drift velocity, given by (68). However

$$\underset{\sim}{M} = - \frac{n\, m\, v_{\perp}^2}{2\, B} \hat{\underset{\sim}{B}} \tag{77}$$

$$\nabla \times \underset{\sim}{M} = - \frac{n\, m\, v_{\perp}^2}{2\, B^2} \hat{\underset{\sim}{B}} \times \nabla B \tag{78}$$

and $\underset{\sim}{j}_{\perp}$ of (74) vanishes (this still holds if populations of this kind with different $v_{\perp}$ are superposed). Thus $\underset{\sim}{V} = 0$ while clearly $\langle \underset{\sim}{v}_d \rangle \neq 0$.

THE OBSERVED VALUE OF ϵ

Bowling and Wolf [1974] have concluded from observations that at 30 R_E the average thickness of the plasma sheet is ≈ 2.5 R_E , over which B_x changes from 10 γ to - 10 γ . This implies

$$\lambda = 2\,\partial B_x/\partial z \approx 16\ \gamma/R_E \tag{79}$$

On the other hand, Behannon [1970] reports that at 30 R_E , $B_z \approx 1.87\ \gamma$, and that the average value of B_z changes from $x = -20\ R_E$ to $x = -40\ R_E$ (x being negative on the nightside) by about 2.5 γ , giving

$$k = 2\,\partial B_z/\partial x \approx 0.25\ \gamma/R_E \tag{80}$$

Thus $\epsilon \approx 1/64$, which means that the order of approximation used here is indeed an appropriate one for the geomagnetic tail at 30 R_E . At $x = -20\ R_E$ the plasma sheet is about twice as thick, suggesting λ is close to half its above value, while k [Behannon, 1970] is about twice the value of (80) : ϵ is thus considerably larger, but the approximation will still hold.

GENERALIZATION

One can in principle extend the preceding calculation to more general fields of the nearly drift-free type, e.g. to fields with B_z as in (2) but with B_x expanded in a more general fashion

$$B_x(z) = \frac{1}{2}\lambda z + c_2 z^2 + c_3 z^3 \quad \ldots \tag{81}$$

where the series is presumed to converge and where even-numbered coefficients vanish in a symmetric configuration. The complexity of the calculation, however, increases rapidly with the addition of terms, and the use of numerical formulas such as (65), with appropriate generalizations of (72) and (73), may well be quicker and less prone to errors than an analytical approach. Here we shall sketch out one relatively simple generalization -- the derivation of the bounce time τ in drift-free fields $(B_z = B_o = \text{const.})$ where B_x has the more general expansion (81). To keep the calculation short we will also assume that all even powers in (81) vanish, so that all bounce-time integrals reduce to 4 times the integral between $z = 0$ and the mirror point on either side. Thus

$$\underset{\sim}{B} = B_x(z)\,\hat{\underset{\sim}{x}} + B_o\,\hat{\underset{\sim}{z}} \tag{82}$$

Dividing by B_o and introducing new variables

$$\underset{\sim}{u} = u_x(z)\,\hat{\underset{\sim}{x}} + \hat{\underset{\sim}{z}} \tag{83}$$

By (7), and with the notation used earlier, this gives

$$\tau = \oint ds/v_{\parallel}$$

$$= (4\, u_m^{1/2} / v) \int_1^{u_m} (u_m - u)^{-1/2}\, u\, (\partial z/\partial u)\big|_{\alpha}\, du \qquad (\quad)$$

Let the function $B_x(z)$ in (81) have an inverse

$$z(B_x) = \sum_{k=1} a_k B_x^k \tag{84}$$

where again in the symmetric case k only takes odd values, since z and B_x reverse signs together, and where $a_1 = 2/\lambda$. Defining L and ζ as in (34),(36)

$$\zeta = \sum A_k u_x^k = \sum A_k (u^2 - 1)^{k/2} \tag{85}$$

where

$$A_k = \lambda a_k B_o^{k-1} \tag{86}$$

Thus

$$dz/du = (1/\lambda)\, d\zeta/du = \sum k A_k u (u^2 - 1)^{(k/2 - 1)} \tag{87}$$

Defining t_o as in (62)

$$\tau = 4 t_o u_m^{1/2} \sum_{k=1} k A_k T_k(u_m) \tag{88}$$

where

$$T_k = \int_1^{u_m} (u_m - u)^{-1/2} u^2 (u^2 - 1)^{(k-2)/2} du \tag{89}$$

Because k is odd, any T_k (except for T_1, which appears in (29) and which has been derived earlier) may be expressed as a linear combination of integrals of the type

$$V_k = \int_1^{u_m} \left[(u^2 - 1)/(u_m - u)\right]^{1/2} u^k du \qquad (\quad)$$

e.g.

$$T_3 = V_2$$

$$T_5 = V_4 - V_2$$

By equations (A-8) and (A-6) these integrals can be expressed in terms of the integrals S_k of appendix A , using the relation

$$V_k = (2/u_m) \left[(k + 5/2)\, S_{k+2} - (k + 3/2)\, S_k \right] \qquad (91)$$

If even-numbered values of k are also allowed in the expansion of B_x, the calculation is modified somewhat and integrals of the type (89) corresponding to even values of k also appear. Such integrals do not have to be expressed in terms of elliptic integrals but instead may be integrated in closed form after a substitution $w = u_m - u$, since their integrand is then a polynomial in w multiplied by $w^{-1/2}$.

CONCLUSION

This work derives for the first time the properties of adiabatic motion in a tail-like two-dimensional magnetic configuration possessing a finite $\partial B_z/\partial x$, which is essential for a net cross-tail drift. It derives instantaneous and average drift velocities, bounce times, longitudinal invariants and approximations to the adiabatic Hamiltonian, and the results are suitably scaled to reduce as much as possible the number of independent parameters.

The mean drift velocity is (as expected) much smaller than the instantaneous drift velocities encountered at typical points on the trajectory. It is comparable to the drift velocity v_o of particles confined to the equatorial plane, which are sensitive only to the small gradient of B_z : as pitch angles decrease, this velocity becomes smaller and for the range investigated here it levels off around $v_o/3$. It is interesting to note that if pairs of neutral points and strong dawn-to-dusk electric fields are formed in the tail during substorms (as is widely believed), the gradient of B_z will reverse its direction on the anti-sunward side of such points and particles drifting there will lose energy to the electric field. This, however, is only expected in a very limited region.

This slow drift suggests that in the plasma sheet of the magnetospheric tail particles advance in the dawn-dusk direction rather slowly, at speeds of the order of 1 - 2 R_E/hour . If an electric field of, say, 40,000 volts exists across the sheet, the earthward convection of such particles will be considerably more rapid. The present calculation does not apply to non-adiabatic protons, which constitute an important part of the plasma sheet's population, but because the present geometry differs only slightly from one which is drift-free even for non-adiabatic orbits [Stern and Palmadesso, 1975] , the cross-tail motion even then is expected to be relatively slow.

It should be readily possible to extend this work to the magnetodisk configuration observed near Jupiter. More generally, the results derived here make available for a tail-like configuration quantities which are already well-known for the dipole case and should make possible the generalization of calculations for the dipole geometry to such configurations as well.

Appendix A : A CLASS OF INTEGRALS

In the study of particle motion in nearly drift free configurations one frequently encounters integrals of the form

$$S_k(u_m) = \int_1^{u_m} u^k \left(\frac{u_m - u}{u^2 - 1}\right)^{1/2} du \qquad \text{(A-1)}$$

These integrals and their derivatives are readily expressed in terms of complete elliptic integrals $\underline{K}(m)$ and $\underline{E}(m)$ of the first and second kind [e.g. Milne-Thomson, 1964] , of the argument

$$m = \left[(u_m - 1)/(u_m + 1)\right]^{1/2} \qquad \text{(A-2)}$$

In what follows, unless otherwise is stated, $\underline{K}$ and $\underline{E}$ will be understood to be evaluated for the above argument. The first two integrals of this type, corresponding to $k = 0$ and 1 , may be expressed by standard substitutions or by consulting tables (Gradshteyn and Ryzhik [1965] , integrals 3.141.4, 3.141.22 and 3.141.23); in either case one finds

$$S_o = 2\,(u_m + 1)^{1/2}\;(\underline{K} - \underline{E}) \qquad \text{(A-3)}$$

$$S_1 = (2/3)\,(u_m + 1)^{1/2}\,(u_m \underline{E} - \underline{K}) \qquad \text{(A-4)}$$

For higher values of k a recursion formula may be developed. Let

$$Q_k = \int \left[(u^2 - 1)(u_m - u)\right]^{1/2} u^k \, du \qquad \text{(A-5)}$$

where the implied limits of integration, here and in subsequent formulas, are always those of (A-1) . Multiplying numerator and denominator by $(u^2 - 1)$ then gives

$$Q_{k-2} = S_k - S_{k-2} \tag{A-6}$$

On the other hand, integrating (A-1) by parts

$$S_k = \int u^{k-1} (u_m - u)^{1/2} \, d\left[(u^2 - 1)^{1/2}\right]$$

$$= - (k - \tfrac{1}{2}) Q_{k-2} + (u_m/2) V_{k-2} \tag{A-7}$$

where V_{k-2} is defined in (90) and may be integrated by parts

$$V_{k-2} = -2 \int (u^2 - 1) u^{k-2} \, d\left[(u_m - u)^{1/2}\right]$$

$$= 2 (k - 2) Q_{k-3} + 2 S_{k-1} \tag{A-8}$$

Substituting the last three equations in a way that eliminates all integrals not of the form (A-1) yields the recursion

$$(k + \tfrac{1}{2}) S_k = u_m (k - 1) S_{k-1} + (k - \tfrac{1}{2}) S_{k-2} - u_m (k - 2) S_{k-3} \tag{A-9}$$

For $k = 2$ the last term drops and one obtains

$$S_2 = (2/5) u_m S_1 + (3/2) S_0$$

$$= (2/15) (u_m + 1)^{1/2} \left[\underline{E} (2 u_m^2 - 9) + \underline{K} (9 - 2 u_m) \right] \tag{A-10}$$

To obtain dS_2/du_m one differentiates beneath the integral sign, noting that the contribution from the upper limit vanishes. The result is equation (30) which has already been analyzed, giving

$$dS_2/du_m = S_1 + (u_m + 1)^{-1/2} \underline{K}$$

$$= (2/3)(u_m + 1)^{1/2} u_m \underline{E} + 3(u_m + 1)^{-1/2}(1 - 2 u_m) \underline{K} \tag{A-11}$$

Performing the same steps for arbitrary k

$$dS_k/du_m = 1/2 \int u^k \left[(u^2 - 1)(u_m - u)\right]^{-1/2} du$$

$$= (1/2)\ dS_{k-2}/du_m + V_{k-2} \qquad \text{(A-12)}$$

One can now express V_{k-2} by means of (91) and thus obtain a recursion for dS_k/du_m. For even values of k the recursion begins with (A-11); for odd values one needs dS_1/du_m, which can be obtained either by standard substitutions or from tabulations (Gradshteyn and Ryzhik [1965], integral 3.132.5). In either case

$$dS_1/du_m = (u_m + 1)^{1/2}\, \underline{E} - (u_m + 1)^{-1/2}\, \underline{K} \qquad \text{(A-13)}$$

Appendix B : INTEGRATION NEAR $u = u_m$

At the mirror point $v_{\parallel} = 0$ and therefore special care is needed when (29) or (65) are integrated near that point. The problem resembles the evaluation of integrals of the form

$$\int_0^A f(X)\, X^{-1/2}\, dX \qquad \text{(B-1)}$$

near their lower limit and there exist various advanced methods for handling it [Smith and Bewtra, 1976]. In this work a rather crude but effective approach is used, as follows.

Consider the evaluation of (B-1): one first divides the range into two parts, the main range $B < X < A$ which is handled by conventional methods (e.g. Simpson's rule) and the end region $0 < X < B$. In that region $f(X)$ is approximated by a polynomial

$$f(X) \approx f(0) + a\,X + b\,X^2 \qquad \text{(B-2)}$$

from which the region's contribution to the integral is found at once to be very nearly

$$2\;B^{1/2}\;(\,f(0) + a\,B/3 + b\,B^2/5\,) \qquad \text{(B-3)}$$

The coefficients a and b can be evaluated using $f(B)$ and some intermediate value $f(C)$, $0<C<B$, but computing time is saved if one directly evaluates aB and bB^2, which appear in (B-3). An alternative approach first removes the singularity in (B-1) by transforming to a new variable $w = X^{1/2}$. If f is then expanded in even powers of w, (B-3) is obtained; if odd powers are also allowed, the result is the same as when both integral and half integral powers are used in (B-2).

The integrals (29) and (65) readily reduce to the form (B-1) if one sets $X = u_m - u$. Note that over the end region (but not over the main range) (65) must first be transformed into an integral over u , after which one introduces $dX = - du$; by (42) and (36a) this requires the addition of a factor

$$\left|\frac{\partial z}{\partial u}\right|_{\alpha} = \frac{4 u L^2}{z (1 + \mathcal{E})} \qquad \text{(B-4)}$$

The above factor contributes to $f(X)$, but since $f(X)$ is used only numerically, z does not have to be expressed in terms of u and the above factor can be used in the form given in (B-4).

REFERENCES

Behannon, K.W., Geometry of the Geomagnetic tail, J. Geophys. Res., 75, 743-753, 1970.

Bowling, S.B. and R.A. Wolf, The motion and magnetic structure of the plasma sheet near 30 R_E, Planet. Space Sci., 22, 673-686, 1974.

Chen, A.J. and D.P. Stern, Adiabatic Hamiltonian of charged particle motion in a dipole field, J. Geophys. Res., 80, 690-693, 1975.

Gradshteyn, I.S. and I.M. Ryzhik, Table of Integrals, Series and Products, translated from the 4th Russian edition by A Jeffrey, Academic Press, 1965.

Milne-Thomson, L.M., Elliptic integrals, in Handbook of Mathematical Functions, M. Abramowitz and I.A. Stegun, editors, U.S. Govt. Printing Office, 1964, pp. 587-626.

Northrop, T.G. and E. Teller, Stability of the adiabatic motion of charged particles in the earth's field, Phys. Rev., 117, 210-225, 1960.

Schatten, K.H., Current sheet magnetic model for the solar corona, Cosmic Electrodynamics, 2, 232-245, 1971.

Schulz, M. Approximate second invariant for a dipole field, J. Geophys. Res., 76, 3144-3148, 1971.

Smith, E.J., B.T. Tsurutani and R.L. Rosenberg, Pioneer 11 observations of the interplanetary sector structure up to 16° heliographic latitude (abstract SS-8), EOS, 57, 997, 1976.

Smith, P.H. and N.K. Bewtra, Dependence of charge exchange lifetimes on mirror latitude, Geophys. Res. Lett., 3, 689-692, 1976.

Stern, D.P. and P. Palmadesso, Drift-free magnetic geometries in adiabatic motion, J. Geophys. Res., 80, 4244-4248, 1975.

Taylor, J.B., Equilibrium and stability of plasma in arbitrary mirror fields, Phys. Fluids, 7, 767-773, 1964.

CAPTIONS TO FIGURES

Figure 1 -- Schematic view of the motion of a charged particle in a drift-free magnetic field of the type discussed in this work.

Figure 2 -- The configuration of a magnetic field line (left scale, lower curve) and the variation along it of $u = B/B_0$ (right scale, upper curve) in the limit $\mathcal{E} = 0$. Both x and z are normalized in accordance with (36).

Figure 3 -- The variation of the mean drift velocity, in units of the equatorial drift velocity v_0, as a function of $u = B/B_0$.

Figure 4 -- The quarter-bounce time, in the normalized units of Table 1, as a function of $u = B/B_0$.

Figure 5 -- The field line of Table 2, divided into segments each of which corresponds to $\Delta z = 0.05$ (normalized units). Drawn at the end of each segment is a line proportional to the net distance covered by guiding center drifts during the particle's traversal of the segment (actually, the displacement should be orthogonal to the drawing). The net displacement for the entire quarter period is about equal to the lowest displacement drawn (but in the opposite direction); the time spent traversing that first segment, however, is only about 1/50 of the quarter-period.

ξ	ζ	u	$\langle v_y \rangle$	$\langle v_y \rangle \tau/4$		$\tau/4$	
				analyt.	numerical	analyt.	numerical
0.010	0.2	1.005	0.993	4.440	4.35	4.474	4.42
0.040	0.4	1.020	0.971	4.433	4.40	4.566	4.54
0.090	0.6	1.044	0.937	4.424	4.39	4.719	4.69
0.160	0.8	1.078	0.895	4.416	4.38	4.932	4.91
0.250	1.0	1.119	0.848	4.414	4.38	5.205	5.18
0.360	1.2	1.168	0.799	4.423	4.38	5.535	5.50
0.489	1.4	1.223	0.751	4.445	4.40	5.922	5.89
0.639	1.6	1.283	0.704	4.484	4.43	6.366	6.32
0.900	1.9	1.383	0.642	4.581	4.52	7.135	7.08
1.206	2.2	1.491	0.589	4.727	4.65	8.026	7.96
1.556	2.5	1.606	0.545	4.928	4.83	9.039	8.95
1.950	2.8	1.726	0.510	5.184	5.07	10.172	10.06
2.388	3.1	1.851	0.481	5.497	5.36	11.425	11.29
2.869	3.4	1.980	0.458	5.867	5.70	12.797	12.63
3.393	3.7	2.111	0.440	6.293	6.09	14.288	14.07
3.960	4.0	2.245	0.426	6.775	6.53	15.898	15.63
6.646	5.2	2.798	0.393	9.259	8.77	23.531	22.94
9.978	6.4	3.367	0.381	12.605	11.69	33.073	31.90
13.919	7.6	3.947	0.377	16.788	15.20	44.529	42.40
18.423	8.8	4.533	0.376	21.793	19.19	57.901	54.35
23.438	10.0	5.122	0.377	27.607	23.59	73.193	67.63

Table 1

x	z	u	$\frac{v_y}{v_\parallel} \frac{ds}{dz} \Delta z$	Δt	$\sum \Delta t$
0.0006	0.05	1.0003	- 4.35	0.1173	0.2345
0.0056	0.15	1.0028	- 4.25	0.1183	0.4704
0.0156	0.25	1.0079	- 4.04	0.1202	0.7097
0.0306	0.35	1.0153	- 3.73	0.1233	0.9545
0.0506	0.45	1.0252	- 3.33	0.1275	1.2073
0.0756	0.55	1.0375	- 2.84	0.1332	1.4708
0.1056	0.65	1.0520	- 2.26	0.1407	1.7482
0.1406	0.75	1.0687	- 1.59	0.1505	2.0439
0.1805	0.85	1.0874	- 0.81	0.1633	2.3637
0.2255	0.95	1.1081	0.10	0.1808	2.7158
0.2754	1.05	1.1307	1.20	0.2058	3.1137
0.3304	1.15	1.1550	2.65	0.2450	3.5816
0.3902	1.25	1.1809	4.91	0.3189	4.1755
0.4551	1.35	1.2084	11.16	0.5574	5.1253
0.4894	1.40	1.2227	mirror point		5.922

Table 2

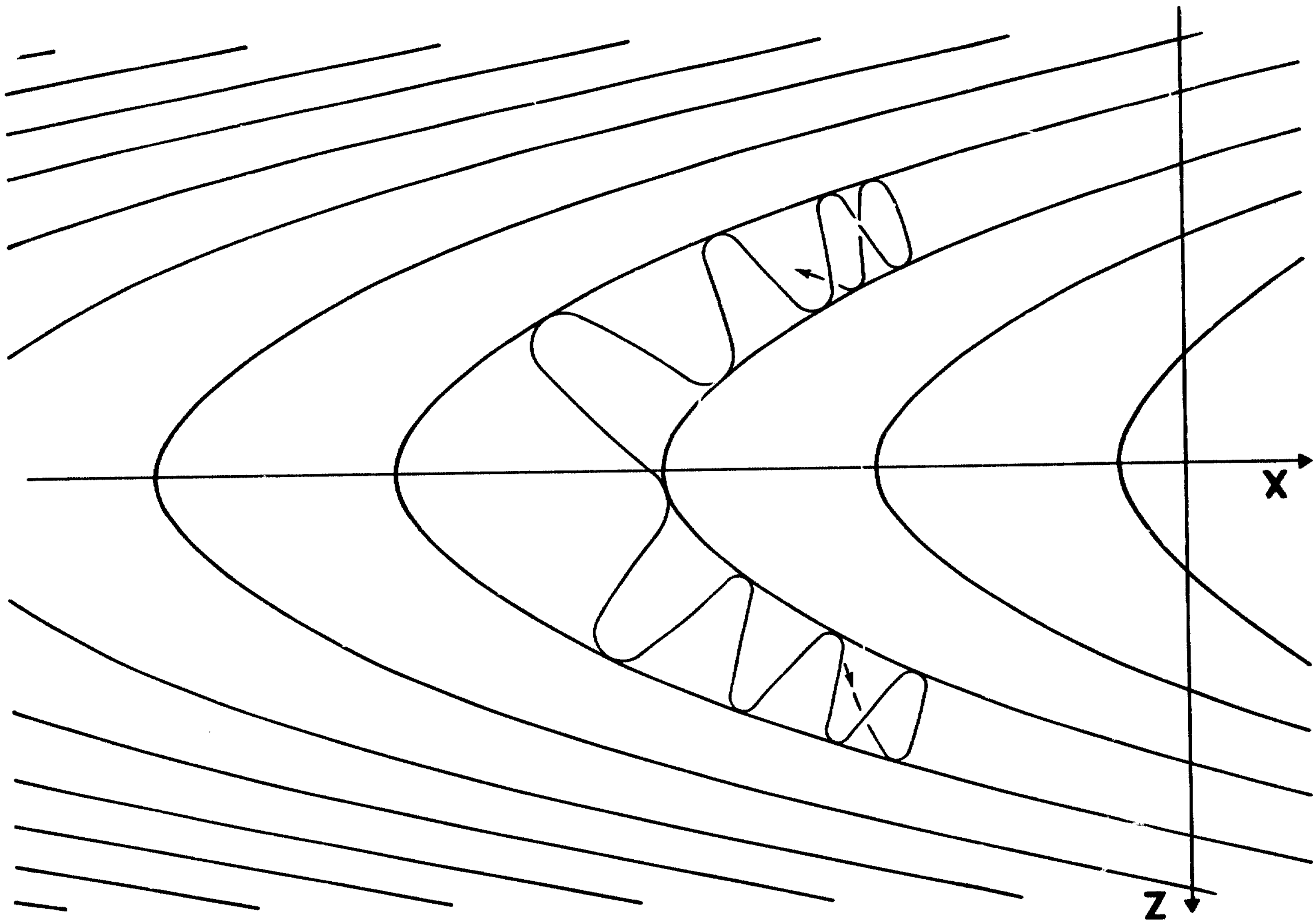

Figure 1

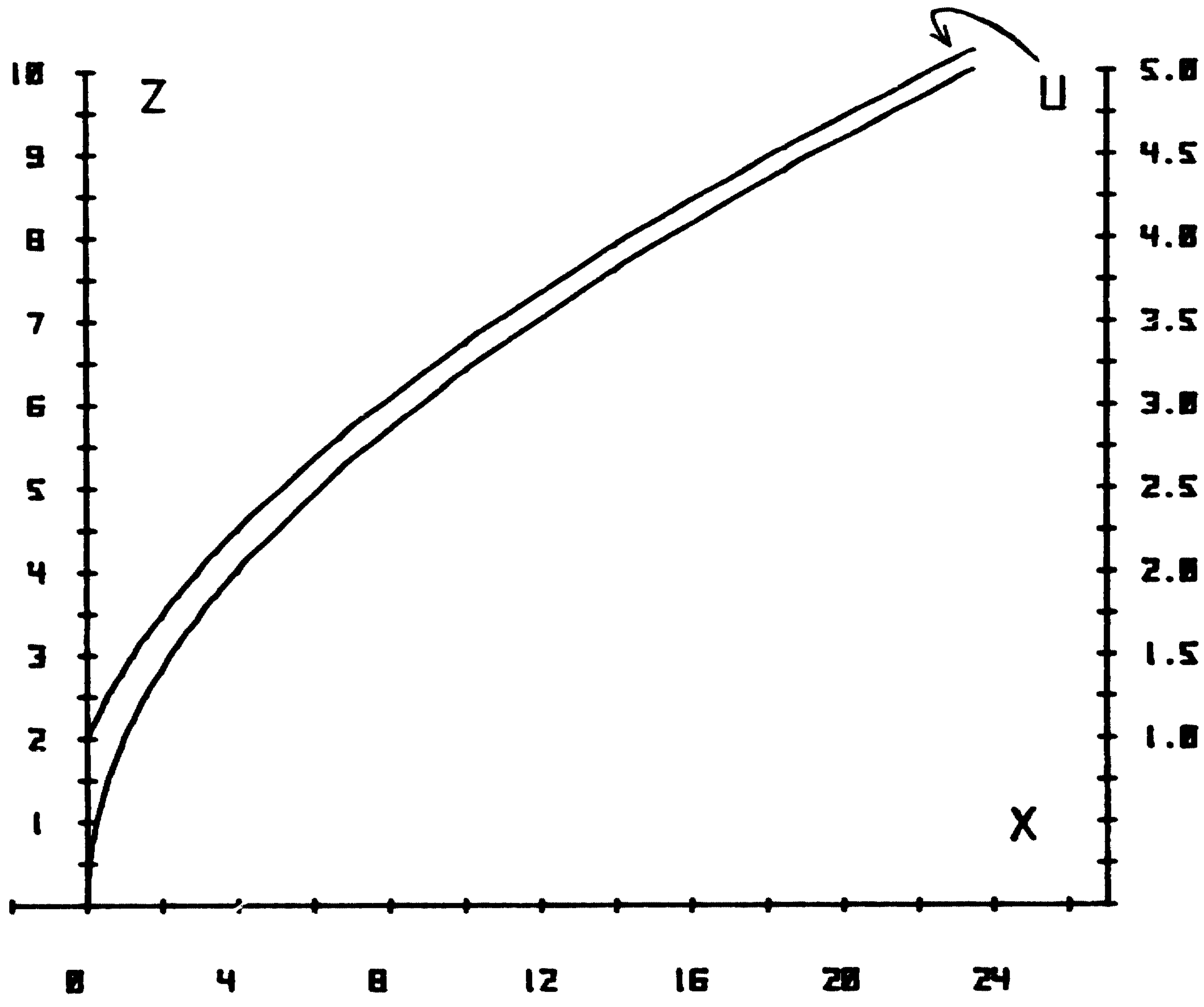

Figure 2

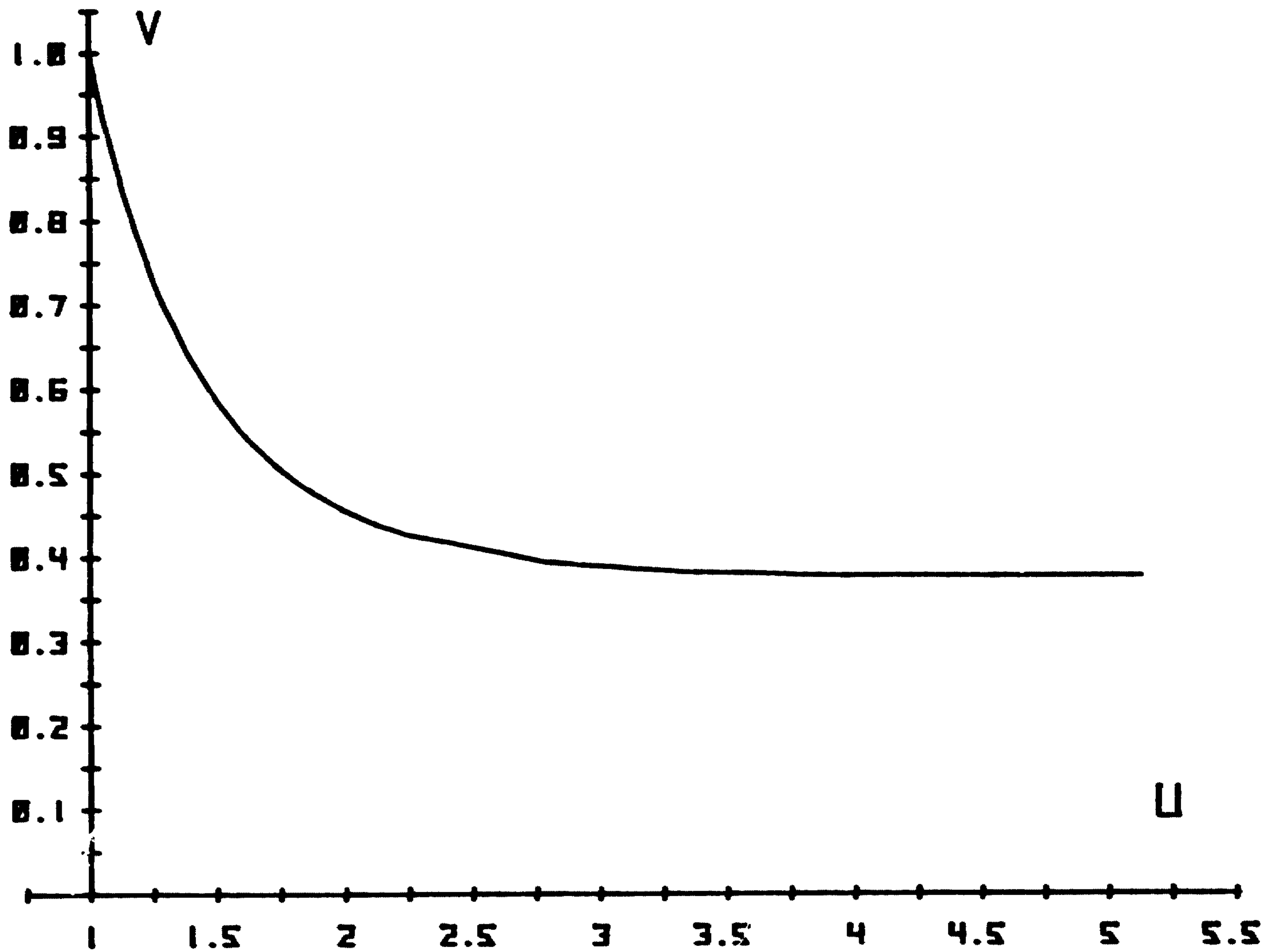

Figure 3

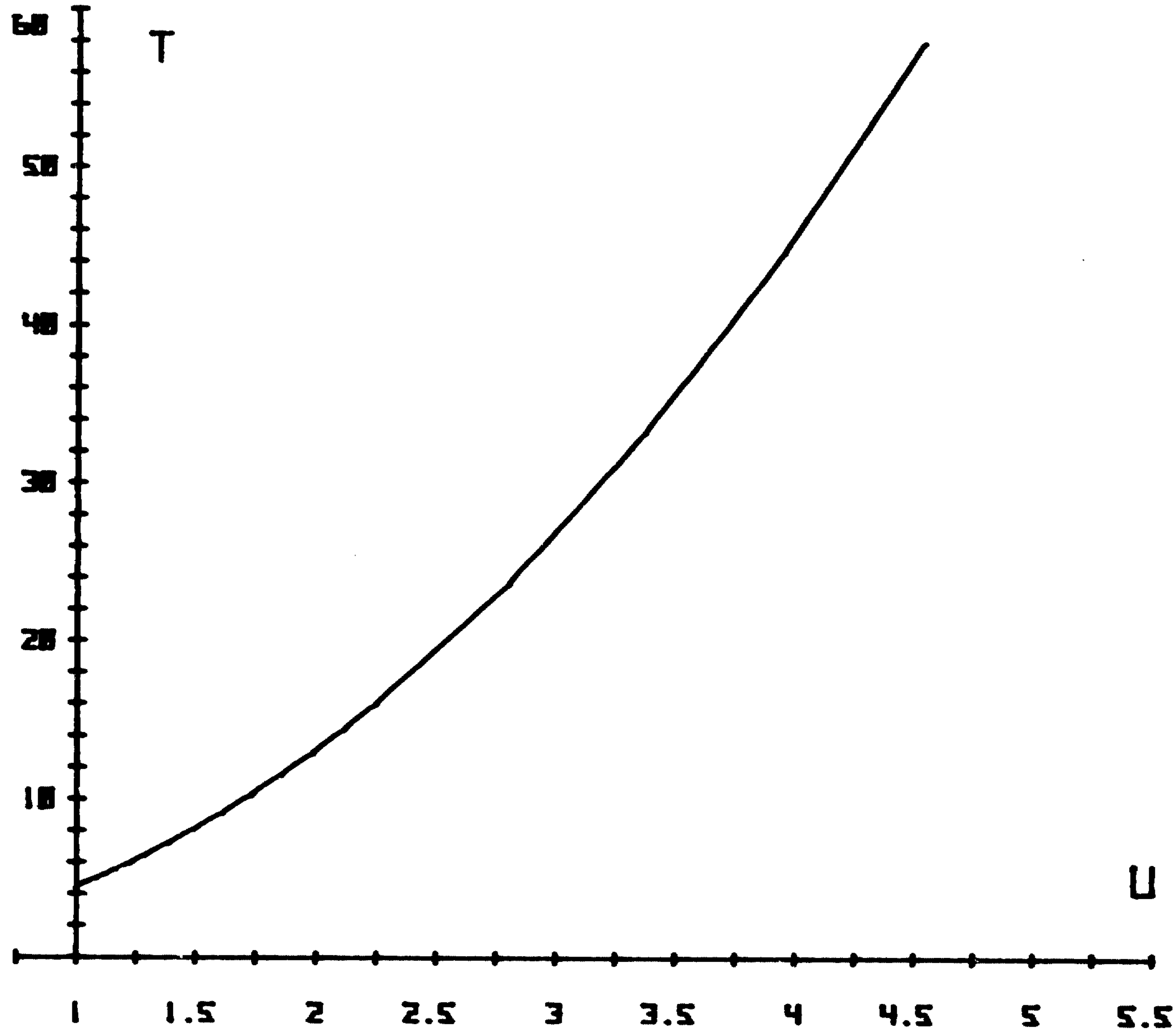

Figure 4

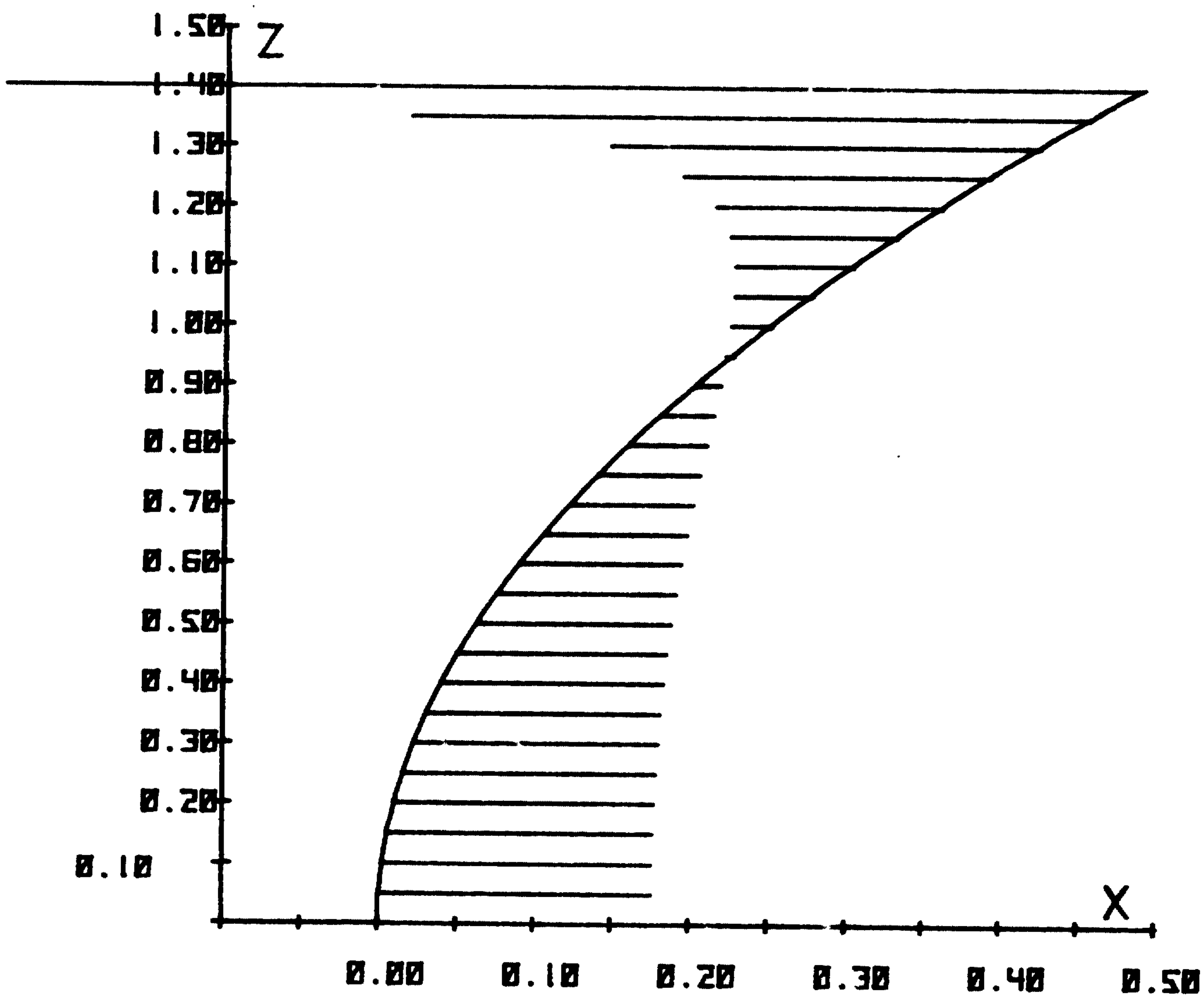
Z
1.50
1.40
1.30
1.20
1.10
1.00
0.90
0.80
0.70
0.60
0.50
0.40
0.30
0.20
0.10
X
0.00
0.10
0.20
0.30
0.40
0.50

Figure 5